Accepted Manuscript

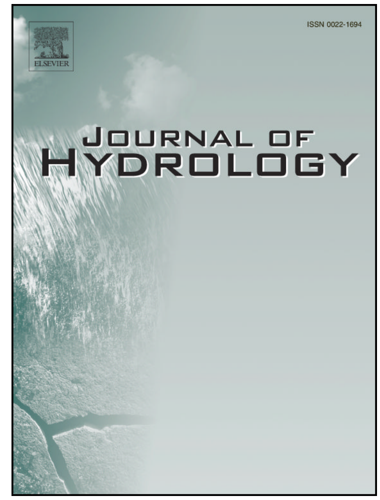

Research papers

Climate change impacts on Three Gorges Reservoir impoundment and hydropower generation

Pengcheng Qin, Hongmei Xu, Min Liu, Liangmin Du, Chan Xiao, Lüliu Liu, Brian Tarroja

PII: S0022-1694(19)30642-0
DOI: https://doi.org/10.1016/j.jhydrol.2019.123922
Article Number: 123922
Reference: HYDROL 123922

To appear in: *Journal of Hydrology*

Received Date: 27 November 2018
Revised Date: 2 July 2019
Accepted Date: 3 July 2019

Climate change impacts on Three Gorges Reservoir impoundment and hydropower generation

Pengcheng Qin[a,b], Hongmei Xu[c,*], Min Liu[a,b], Liangmin Du[a,b], Chan Xiao[c,*], Lüliu Liu[c], Brian Tarroja[d,e]

[a] Wuhan Regional Climate Centre, Hubei Meteorology Bureau, Wuhan, China

[b] Hubei Key Laboratory for Heavy Rain Monitoring and Warning Research, Institute of Heavy Rain, China Meteorological Administration, Wuhan, China

[c] National Climate Centre, China Meteorological Administration, Beijing, China

[d] Advanced Power and Energy Program, University of California – Irvine, Engineering Laboratory Facility, Irvine, CA, USA

[e] Department of Civil and Environmental Engineering, University of California – Irvine, Irvine, CA, USA

* Corresponding author.

E-mail addresses: qinpengcheng027@163.com (Qin, PC), xuhm@cma.gov.cn (Xu, HM), liuminccg@sohu.com (Liu, M), duliangmin@gmail.com (Du, LM), xiaochan@cma.gov.cn (Xiao, C), liull@cma.gov.cn (Liu, LL), bjt@apep.uci.edu (Tarroja, B)

Abstract Climate change is expected to alter regional hydrological regimes, affecting the operation and performance of reservoirs and hydropower facilities. This study examines the impacts of climate change on the performance of the Three Gorges Reservoir (TGR) by means of a detailed daily reservoir regulation and hydropower model, linked to a physically-based hydrological model, and driven by an ensemble of five General Circulation Models (GCMs) under three Representative Concentration Pathways (RCP2.6, RCP4.5 and RCP8.5). As precipitation in the basin is expected to increase, the projected mean annual inflow and hydropower generation of the TGR will increase by 3.3-5.6% and 0.9-2.3% in 2040-2065, 7.9%-15.2% and 5.2-8.1% in 2080-2099 respectively. These increases are only statistically significant for 2080-2099 and are seasonally concentrated in the spring before the flood season and the early autumn during the end of the flood season. However, the inter-annual variation of power generation will increase strongly in the dry season. The reservoir performance is highly sensitive to the changes in the seasonal distribution and extremes of streamflow. Increases in streamflow that occur in the flood season cause significant increases in the amount of spilled water and advance the time when the reservoir reaches the normal storage level. Additionally, increases in both the inter-annual variation of inflow and the intensity of inflow shortages during extreme drought years in the impounding stage drive decreases in the fully filled rate and average water storage level in the dry season. The utilization rate of water resources under projected extreme streamflow is expected to decrease, reshaping the response of power generation to climate change into a non-linear pattern where increases in streamflow do not proportionally translate to increases in power generation. These findings highlight the complexity of hydropower management and production under future climate change scenarios, motivating the need for introducing detailed regulating models for impact assessment studies and adaptive adjustment of the reservoir management to combat climate change.

Keywords: Climate change - Three Gorges Reservoir - Streamflow - Hydropower - SWAT

Highlights:

1) The annual power generation of TGR will increase under climate change.

2) The stability of power generation of TGR will decrease.

3) The response of TGR power generation to streamflow change is non-linear due to hydrological extremes.

4) The future reservoir management for TGR should take adaptive measures to deal with the flood and reduce the spilled water.

1. Introduction and Background

Climate change caused by the emission of greenhouse gases (GHG) is accelerating the global water cycle by increasing evaporation and precipitation rates (Syed et al., 2010; Huntington et al., 2018), consequently redistributing water resources and exacerbating the severity and occurrence of extreme hydrological events (Loaiciga et al., 1996; Syed et al., 2010). This will significantly affect the operation of water resource infrastructure such as reservoirs and hydropower production (Ehsani et al., 2017; Turner et al., 2017a; van Vliet et al., 2016). The increasing demand for energy to support socioeconomic development, however, will drive continued increases in emissions and the atmospheric concentrations of GHGs, resulting in a more dramatic change in the climate and hydrological regime in the 21st century (IPCC, 2014). On the other hand, as a dominant and low-cost renewable source of energy, hydropower plays a vital role in reducing GHG emissions and mitigating climate change and is experiencing vigorous expansion in many regions of the world (Berga, 2016).

Numerous studies have investigated climate change impacts on water resources and hydropower generation, most of which employed a top-down modeling approach using projections from general circulation models (GCMs) integrated with one or more hydrological models and reservoir operation and hydropower models (Turner et al., 2017a; van Vliet et al., 2016; Zhou et al., 2015). It was generally found that at the global scale, the projected annual mean streamflow will increase in high-latitude and wet tropical regions, decrease in most dry tropical regions, and hydrological extremes will become more frequent (IPCC, 2014). The altered spatial and temporal distribution of streamflow will therefore affect hydropower production, with a net global decrease in the 21st century under RCP2.6 and RCP8.5 reported by van Vliet et al. (2016), and only small parts of the world experiencing an increase in hydropower production including Canada, northern Europe, Central Africa, India, and northeastern China. Another recently reported global scale assessment conducted by Turner et al. (2017a) indicated that globally aggregated hydropower production will change by −5% to +5% by the 2080s under a high emissions scenario, with the central Asia and Scandinavia experiencing increases due to climate change. A range of national, regional, and site-specific studies have also been conducted elsewhere in the world (Bartos and Chester, 2015; de Queiroz et al., 2016; Gaudard et al., 2014; Kao et al., 2015; Liu et al., 2016; Majone et al., 2016; Maran et al., 2014; Mendes et al., 2017; Savelsberg et al., 2018; Tarroja et al., 2016; Vicuña et al., 2011). Despite the large uncertainties sourced from emission scenarios, GCMs, and hydrological models (Woldemeskel et al., 2014; Carvajal et al., 2017; Chilkoti et al., 2017), the impacts of climate change on hydrological processes and the water resource system varies widely by region. These will depend on local climate change effects, topographic features, and the local structure of water resource management infrastructure and practices.

The Three Gorges Reservoir (TGR), located at upstream of Yangtze River in China, is the world's largest hydroelectric power plant in terms of installed capacity. The TGR has a dam height of 185 m and is designed to withstand a normal pool level of 175 m with a storage capacity of 39.3 billion m^3 (Niu, 2016). The total installed power capacity of the TGR is 22,500 MW from 34 stand-alone turbines, and has provided an average yearly production of 92.0 TWh since 2012. The capacity factor is only 46.7%, leaving much potential untapped. Due to large annual and inter-annual variations in the inflow with a monsoon climate in the upstream catchment, the main function of the TGR is flood control. Therefore, it must be operated at a low storage level during the flood season, with operation levels increased gradually after the flood season. As a result, the power production, as well as the overall benefits of the TGR are highly dependent on the upstream inflow, which is influenced by the climatic conditions.

Long term historical runoff of the TGR basin has been thoroughly investigated, and studies have also shown that future runoff patterns are expected to change significantly. Runoff observations at the Yichang hydrology station, located 48 km downstream of the TGR, can be traced back to 1877. Analysis of the Yichang station runoff sequence in the last 120 years shows that the annual minimum runoff and average runoff decreased by 6% and 8% respectively (Xiong and Guo, 2004), and the downward trend of average runoff in the last 60 years is more significant (Zhang et al., 2016). Over the same time period, the annual distribution of runoff showed a homogenization trend (Zhang et al., 2016). Studies show that on a 100-year scale, the change in runoff is mainly controlled by climate change with human activity only affecting the annual distribution of runoff in this basin (Liu and Du, 2017). In recent years, however, the construction of upstream water conservancy projects and the increase of water demand have increased the influence of human activities on runoff (Zhang et al., 2016). Many studies have also assessed future climate change impacts on runoff in the upper catchment of the TGR. Sun et al. (2013) and Wang et al. (2015) studied the spatiotemporal change of streamflow in the upstream Yangtze River in response to climate change under Special Report on Emissions Scenarios (SRES) reported by the Intergovernmental Panel on Climate Change (IPCC) in the Fourth Assessment Reports. These studies showed that streamflow in the Yangtze will decrease in the 21st century due to decreases in precipitation. Gu et al. (2015) reported that the frequency of extreme floods in the upstream Yangtze River is projected to increase significantly at the end of the 21st century under SRES scenarios. Su et al. (2017) and Chen et al. (2017) assessed the impact of climate change on river discharge in the upper reaches of the Yangtze River, using five GCMs from Phase 5 of the Coupled Model Intercomparison Project (CMIP5) under the newest Representative Concentration Pathways (RCPs) adopted by the IPCC in its Fifth Assessment Report. These studies concluded that the annual runoff, flood season maximum runoff, and daily runoff peak would increase due to increases in predicted precipitation in the 21st century. By contrast, Birkinshaw et al. (2017) used 78 climate model projections from CMIP5 and found that in RCP8.5 case, precipitation in the upstream of the TGR increased by 4.1% in 2041-2070, but the upper streamflow of the TGR still decreased by 11.1% due to the significant increase of evapotranspiration caused by the rising temperature. Therefore, it can be seen that there is still great uncertainty on the estimated streamflow of the TGR under future climate change.

Relatively few studies have focused on the reservoir performance and hydropower production of the TGR under climate change. Some existing studies have assessed the impact of climate change on hydropower output in China as a whole as well as specifically in China's Yangtze River basin, including the TGR from a macro perspective (Fan et al., 2018; Liu et al., 2016; Zhang et al., 2017; Zhou et al., 2015). These results show that China's hydropower output declines in the first half of the 21st century and increases in the second half of the 21st century, hydropower output in northern China primarily increases while that in southern China (including the TGR) primarily decreases, and the hydropower variation is consistent with that of annual runoff caused by climate change. These studies provide important references for forming China's energy development planning and GHG emission reduction policies. However, large scale macro studies have to adopt general and simplified schemes for reservoir operation (Liu et al., 2016; van Vliet et al., 2016; Zhou et al., 2015), ignoring the specific important features of individual reservoirs, which may cause large errors in the estimation of power generation efficiency. Recent studies have shown that the response of hydropower output to climate change can be non-linear if detailed consideration is given to the day-to-day management of reservoirs (Turner et al., 2017a). In addition, the effect of extreme hydrological events on power generation may be underestimated as the assessment time scale is usually in months or years (Naz et al., 2018).

The TGR is responsible for protecting the lives of tens of millions of people downstream, and also provides benefits from power generation, navigation, water supply, and environmental protection. Therefore, TGR scheduling decisions are affected by multiple objectives. The response of reservoir performance, especially of hydropower generation to changes in climate, is far more complicated than other reservoirs (Jahandideh-Tehrani et al., 2015; Rheinheimer and Viers, 2015; Shang et al., 2018). This study aims to systematically assess the impact of climate change on the performance of the TGR following a hydrological-electricity modeling framework forced by conventional GCMs (Carvajal et al., 2017; van Vliet et al., 2016), specifically with a detailed and realistic reservoir operation simulation at daily scale. The novelty and primary contribution of this study is to highlight complexities in the response of the multi-purpose TGR reservoir to climate change impacts that have not been previously captured in the literature, which has primarily focused on macro-scale analyses for this region. Specifically, this study will illuminate the role of multiple reservoir constraints or priorities in shaping how a multi-purpose reservoir responds to climate change. This provides insight into the potential benefits of TGR management in future climate scenarios as well as how lessons for how these management practices may need to be altered to better adapt to climate change.

2. The Three Gorges Reservoir – Overview and Operating Rules

The TGR controls a catchment area about 1 million km^2, ranging from 90°33'E to 111°39'E and 24°21'N to 35°52'N, with a large topographic gradient across 200 to 6,500 m (Fig. 1). The average annual precipitation of the basin ranges between 723 to 1,134 mm, the average annual temperature ranges between 8.6 to 16.8^{o}C, and the annual runoff is about 400 billion m^3. Influenced by the East Asian monsoon, South Asian monsoon, and the topography of Tibetan plateau, the climate and hydrological characteristics have obvious seasonal changes. About 80 percent of the annual precipitation and 70 percent of the annual runoff are concentrated in the flood season (from May to September), causing many heavy rains and floods. In contrast, the proportion of precipitation and runoff in the dry-season is relatively small.

FIGURE 1

As a key control and multi-purpose hydro-development project in the upper Yangtze River, there are strict operation rules for the TGR (Niu, 2016; Shang et al., 2018). Generally, the operation of the TGR can be divided into four stages during a hydrological year: flood control, impounding, normal pool level, and falling stage (Fig. 2). From June 10 to September 10, the reservoir level is maintained at a flood limiting level of 145 m. When the inflow is less than 35,000 m^3/s, water is completely released. Otherwise, flood control operations are conducted considering the downstream safety and release capacity of hydro turbines. Once a flood process recedes, the water level must drop to 145 m. The impounding stage begins at the end of the flood season, with the water level gradually rising to no more than 162 m at the end of September, and to 175 m no earlier than the end of October. From November to December, the reservoir water level should be kept as high as possible if the storage level has already reached the final stage of 175 m, otherwise, the water level should continue to rise until up to 175 m. Considering the need for navigation and water supply downstream, the minimum release should be no less than 8,000 m^3/s when the inflow is less than 10,000 m^3/s in September, and no less than 10,000 m^3/s when the inflow is more than 10,000 m^3/s in September. In October, the minimum release should be no less than 8,000 m^3/s when the inflow is more than 8,000 m^3/s. In November and December, the release should be no less than 5,300 to 6,460 m^3/s. For special years when the inflow is greater than 35,000 m^3/s during the impounding stage, the impoundment should suspend and transfer to flood control operation. From January to early June is the falling stage, with the water level declining steadily to no lower than 155 m at the end of April, no higher than 155 m after May 25, and further declining to the base level of 145 m before the flood season. In order to satisfy navigation demands, ecological protection, and water resource utilization downstream, the minimum release should be no less than 6,000 m^3/s during the falling stage. The monthly mean inflow, water height, and power generation during a year are listed in Table 1.

FIGURE 2

TABLE 1

3. Data and Methodology

3.1 Available data

Gridded daily climate data with a spatial resolution of 0.5° obtained from the CN05.1 dataset (Wu and Gao, 2013) was used for the hydrological model calibration and GCMs biases analysis. The dataset was constructed from over 2400 observing stations in China from 1961 to 2017, and has been widely used in assessing global and regional climate model performance (Guo et al., 2017).

Hydrological data were obtained from the Changjiang Water Resources Commission (CWRC). This dataset include: 1) monthly observed and naturalized streamflow from 2000 to 2015 at six key hydrological stations in the TGR basin and 2) measured daily inflow, outflow, and water height at the TGR from 2000 to 2017. The daily hydropower output from 2015 to 2017 and the annual hydropower output from 2012 to 2017 were also collected from China Three Gorges Corporation for the hydropower model calibration.

Climate projections from five GCMs (GFDL-ESM2M, HaDGEM2-ES, IPSL-CM5A-LR, MIROC-ESM-CHEM, and NorESM1-M) under three RCPs (RCP2.6, RCP4.5 and RCP8.5) were obtained from the Inter-Sectoral Impact Model Intercomparison Project (ISI-MIP). The output of these five models was originally derived from the CMIP5 and further downscaled and bias-corrected using a trend-preserving approach with WATCH forcing data at 0.5° spatial resolution (Hempel et al., 2013). Data were divided into a historical baseline period of 1986-2005 and two future periods (2046-2065 and 2080-2099) in order to quantify the impacts of future climate change scenarios. Summary of the ensemble climate projections are listed in Table 2, and detailed magnitude and statistical significance of the changes detected relative to the baseline period for each GCM are presented in Fig. S1-S2 of the Supplementary Material. For temperature, significant, uniform increases are projected for both future time horizons and all GCMs. For precipitation, all of the GCMs except for HaDGEM2-ES projected weak but not statistically significant increases for 2040-2065, while significant increases in 2080-2099 are expected for all the GCMs except for GFDL-ESM2M.

TABLE 2

3.2 Methodology

In this study, a physically-based and semi-distributed hydrological model called the Soil and Water Assessment Tool (SWAT) (Arnold et al., 1998) was employed to simulate streamflow in the catchment upstream of the TGR under historical and future climate scenarios. A simple empirical model was then used to simulate the regulation function of upstream reservoirs, and the natural runoff simulated by SWAT was revised to the TGR inflow. The daily reservoir scheduling of the TGR is then simulated according to the TGR operation rules to obtain the daily discharge and reservoir water level, which are used as input to the hydropower model to obtain power generation. Finally, the impact of climate change is comprehensively evaluated by selecting relevant indicators from such aspects as runoff, reservoir storage and power generation.

3.2.1 Streamflow simulation

To represent streamflow response to climate change, SWAT was run at a daily time step and a 1km^2 spatial resolution. SWAT was first calibrated with the monthly natural streamflow data during 2000-2009, evaluated with data during 2010-2015, and subsequently run for each climate scenarios under different RCPs. Performance of the calibrated SWAT model was evaluated using Nash-Sutcliffe efficiency (NSE) and coefficient of determination (R^2) (Xu et al., 2011; Liu et al., 2017; Mohammed et al., 2017), with a value greater than 0.5 is considered acceptable. Overall, the simulation accuracy is reasonably acceptable (Table 3) with NSE ranging from 0.85 to 0.89 during calibration period, and 0.81 to 0.91 during validation period, R^2 ranging from 0.87 to 0.91 during calibration period, and 0.88 to 0.92 during validation period, no obvious difference was found between calibration and validation period. The SWAT model also closely matches with the well-used Variable Infiltration Capacity (VIC) model for the river basin of interest, discussed later in Section 5.3.

TABLE 3

3.2.2 Reservoir inflow simulation

Many reservoirs have been built upstream of the TGR and many more are currently under construction or have been proposed for construction. By 2016, the accumulated regulated storage capacity of upstream reservoirs has exceeded 52 billion m^3, and the planned total storage capacity will reach 100 billion m^3. Most large reservoirs are capable of seasonal regulation. Flood control is carried out during the rainy season, water is stored at the end of the flood season, and the reservoir level is lowered to the flood control level before the start of the next rainy season (Zhou et al., 2017).

The upstream reservoirs significantly alter the natural inflow of the TGR, flattening the peak inflow during the flood season, and causing higher inflow in the dry season (Zhang et al., 2012). Considering the large numbers of the upstream reservoirs and complexity of the dispatching process, in this study the monthly reservoir inflow model was established based on the regression model using a fitting method (Feng et al., 2017; Young, 1967). Specifically, this is accomplished by generalizing the regulating function of upstream reservoirs into one reservoir and subsequently using a moving average algorithm to smooth the daily flood peak process. Through comparing the flow duration curve (FDC) of simulated and observed inflow with different moving windows, a 15-day duration was determined as the optimal window. Based on this, the natural streamflow simulated by SWAT was converted into daily TGR inflow regulated by upstream reservoirs. Considering the systematic bias between the SWAT simulated streamflow driven by different GCMs and CN05.1, the simulated streamflow for each GCM was first corrected by a scaling factor derived from the ratio of the CN05.1 and GCM-driven streamflow simulations.

A comparison of hydrographs for the monthly observed and simulated reservoir inflow during 2000-2016 is shown in Fig. 3. The simulated inflow matches well with the seasonality of the actual inflow, and the peak flows and low flows during many of the validation years are consistent with the observed data except 2004, 2015 and 2016. The bias in 2015 is related to the simulation bias of the SWAT model, and the bias of other years may be related to reservoir operation management. Although there are strict regulations for reservoir operation, there is still room for adjustments in real-time operation according to the inflow and special demand. In general, the NSE coefficient between simulated and observed inflow is 0.83, with a determination coefficient R^2 of 0.85, indicating a considerably high simulation accuracy. Fig.4 shows the FDC curve of daily observed inflow, SWAT simulated, and further revised with upstream reservoir regulation. Since the regulation of upstream reservoirs was not taken into account, the FDC curve of SWAT simulated inflow is significantly different from that of the observed. The low-frequency flowsimulated by SWAT is significantly higher than that of the observed, while the simulated inflow can reach 135,000 m^3/s, the actual maximum inflow of the TGR is only 68,000 m^3/s, however, after revised by seasonal adjustment and smoothing processing, the simulated inflow is basically close to actual inflow in terms of extreme value distribution, which will not cause much error for the analysis of reservoir storage characteristics and power generation prediction.

FIGURE 3

FIGURE 4

3.2.3 Hydropower electricity simulation

To simulate hydropower electricity output, the reservoir water height and outflow released for hydropower generation in each day is calculated from a mass balance (Ng et al., 2017; Carvajal et al., 2017) based on the previously simulated inflow:

$$S_{t+1} = S_t + Q_t - R_t - E_t \tag{1}$$

$$S_{min} \leq S_t \leq S_{max} \tag{2}$$

$$R_{min} \leq R_t \leq R_{max} \tag{3}$$

where *St* is the reservoir storage; Q_t is the reservoir inflow volume; R_t is the water release volume to the turbines; and E_t is the evaporation loss from the reservoir surface. E_t is neglected on the daily scale since evaporation is very small for the TGR specifically relative to the other factors considered (Sun et al., 2012). S_t is constrained by the maximum storage S_{max} and the minimum storage S_{min}, which dynamically changes during the year depending on the constrained water level of the TGR operating rule curves (Fig. 2). The relationship between reservoir storage and water height was established with the historical observed data using local polynomial regression. R_t is also constrained between a lower bound R_{min} and an upper bound R_{max}, considering the downstream safety and water supply requirements in the lower reaches, previously described in Section 2.

Finally, daily hydropower electricity output in TWh is simulated using the following equation (Carvajal et al., 2017; van Vliet et al., 2016):

$$P = \eta \cdot \rho \cdot g \cdot H \cdot Q \cdot t \cdot \left(\frac{1\ TWh}{10^{12}\ Wh}\right) \tag{4}$$

where Q represents the reservoir outflow through turbines, m^3/s; H is the hydraulic head, m; η is the efficiency of the turbines and generators ranging from 0 to 1; ρ is the water density, 10^3 kg/m^3; g is the acceleration of gravity which is 9.806 m/s^2; t is the time step in hours as used in this study (24 hours); and P is the daily electricity output in TWh. The overall efficiency η is estimated with a fixed value of 0.920, based on two years of electricity output data, the observed daily outflow from the reservoir during 2015-2016, and validation with another year of 2017 (Fig. S3). The hydraulic head H is generally dynamic and can be calculated by the difference of water height between the upstream and downstream of the dam. Since Gezhouba Dam is 38 kilometers downstream of the TGR and has a normal operating water level of 66 m, the hydraulic head H can be generally estimated by the difference in the storage water height of the TGR using Gezhouba Dam as the lower bound. Table S1 lists the hydraulic head corresponding to different reservoir water levels, the minimum outflow for one turbine to operate, and the maximum effective flow rate for running at maximum capacity calculated using equation (4).

Simulated and observed power generation are closely matched (Fig. 5), with an average relative error of only 2.1%. Simulated power generation in 2012 is slightly higher than the observed since the TGR power station was not operated at full capacity until July 2012, and the simulated peak value in the flood season is also slightly higher than the observed (Fig. S3). For the convenience of calculation, the hydropower model of this study adopts a uniform annual comprehensive efficiency coefficient. In practice, the water level difference during TGR operation is large, and the efficiency of power generation under different operating water levels (hydraulic head) will vary, so ideally the efficiency coefficient should be dynamic. The current assumption therefore leads to the overestimation of power generation under low hydraulic head conditions in flood season. Nevertheless, the overall accuracy of the model is still high, and this factor can be ignored compared to the large uncertainties from climate projections and hydrological model.

FIGURE 5

3.2.4 Metrics for assessing and quantifying impacts

This analysis employs a total of 11 metrics for assessing and quantifying the effects of climate change on the performance of the TGR. Four focus on changes in upstream streamflow, three focus on reservoir fill dynamics, and four focus on hydropower generation characteristics.

The natural streamflow upstream of the TGR is the foundation of reservoir storage and power generation. The total runoff directly determines the upper limit of available water resources. In addition, the flood season storage and extremely high or low flow significantly affect the operation and efficiency of the reservoir. Therefore, four flow metrics are selected to measure the gross amount of streamflow and the change in hydrologic extremes under climate change scenarios for the two future time periods: the mean annual flow (MAF), mean flood season flow (MFF), extreme high flow (Q_5), and extreme low flow (Q_{95}). The extreme high and extreme low flows refer to events when the daily flow exceeded 5% and 95% of the time.

The TGR is a seasonal regulating reservoir. The reliability of full storage in the flood recession period and the storage level have an important influence on the benefits provided by this reservoir. In addition, the day when the reservoir storage level reaches the maximum impounding level is important for reservoir operation and scheduling. Therefore, three metrics are selected to examine the impact of climate change on the performance of the reservoir impoundment for the two time periods: Fully filled rate (FFR), defined as the percentage of years where maximum fill level reaches the maximum impounding level of 175 m, mean first full fill day (MFD), defined as the average of the first day in each year that the reservoir storage level reaches 175 m, and mean fill level (MFL) which represents the average maximum fill level for the assessment years.

For hydropower facilities, the total power generation is the main metric of interest, and its inter-annual variation has an important influence on the stability of power supply. In addition, when the reservoir release is lower than the minimum flow demand of the turbine, power generation will cease. When the release is higher than the maximum usable flow, water will be spilled. Both of these events will waste water resources from the perspective of power generation and subsequently decrease the utilization efficiency of water resources. Therefore, the mean annual power (MAP), coefficient of power variation among years (square root of variance/mean; CV), power generation assurance rate (PAR), and spilled water rate (SPW) are analyzed. PAR and SPW are determined by first calculating the ratio of the number of days in the year below the minimum flow demand (for PAR) or above the maximum usable flow (for SPW) to the total number of days for each year, then averaging across all years for the evaluation period. As the hydraulic head varies with reservoir level and leads to different power generation efficiencies, the minimum required and maximum effective flow rate varies with reservoir levels. Both thresholds for any reservoir level can be back-calculated by equation (4), and values under typical reservoir levels are listed in Table S1.

4. Results

4.1 Projected change in streamflow

Table 4 presents the projected change in the ensemble mean and range of streamflow metrics at the TGR basin. The statistical significance of these changes is presented in Fig. S2 in the supplementary material. Generally, the projected change in the ensemble mean of MAF, MFF, Q5, and Q95 all show increasing trends, with the 2080-2099 period being more prominent than that of 2046-2065, while the magnitudes vary across GCMs and RCPs. For MAF, MFF, and Q5, most of the GCMs project an increasing trend under different RCPs, more than half of which is statistically significant in 2080-2099, especially for RCP8.5. The changes projected by most of the GCMs in 2040-2065 are not statistically significant, with the exception of HaDGEM2-ES. For Q95 flow, there is only a slight increasing trend for the ensemble mean of all the GCMs, and both the direction and magnitude of flow change vary significantly across GCMs, indicating large uncertainty.

TABLE 4

Fig. 6 displays the monthly average streamflow variation and the coefficient of variation relative to the reference period under different RCPs in 2046-2065 and 2080-2099. The projected ensemble mean streamflow increases in most months in the two future time horizons, with considerable differences between months in the case of RCP4.5 and RCP8.5. Large increases occur in months before the flood season (March, April, May) and at the end of the flood season (September), and there is also a notable increase in the flood season (June, July, August) in 2080-2099. The inter-annual streamflow variation in each month shows an overall increasing trend, except for the relatively small and even slightly reduced changes in January and April. A large variance occurs in October – December under RCP2.6, in June – October under RCP4.5, and in June – September under RCP8.5. In addition, the coefficient of variation in 2046-2065 is similar to that in 2080-2099.

The change in projected future streamflow varies strongly across GCMs, and there is even no consistency in the direction of change. The GFDL-ESM2M model projects a significant increase of streamflow in the flood season and a decrease in the non-flood season, resulting in a more concentrated streamflow distribution pattern. The inter-annual streamflow variation simulated by GFDL-ESM2M model is always much greater than other GCMs, representing a more extreme climate change scenario. The IPSL-CM5A-LR model, by contrast, shows a small increase or decrease of streamflow in the flood season and an increase in the non-flood season. This model also shows a more moderate and inconsistent direction of change in inter-annual variation, representing a more moderate climate change scenario. The behavior of the other three GCMs is between the previously described models. The HadGEM2-ES model is specifically characterized by a larger increase in streamflow in accordance with precipitation (Fig. S1). Unfortunately, future projections for the study region show a more extreme and fluctuating climate (IPCC, 2013; Deng et al., 2013; Chen et al., 2014; Zhou et al., 2014).

FIGURE 6

4.2 Projected change in reservoir impoundment

Table 5 shows the projected changes in the ensemble mean and range of reservoir storage metrics relative to the reference period under different RCPs. It is observed that the FFR decreases by 0.7-6.7% under all RCPs in 2046-2065 with the largest decline under RCP4.5, and increases by 3.3-7.3% under all RCPs in 2080-2099, with the largest increase under RCP8.5. The MFD is consistently advanced under all

RCPs in both future time horizons, respectively by 2.0-4.7 days and 2.6-8.4 days averaged over GCMs. The MFL shows a decreasing trend, with an average decrease by 0.2-0.6 m in 2046-2065 and by 0.1-0.2 m in 2080-2099. However, the results show a wide spread across GCMs for all the three metrics, without agreement on the direction of change. Detailed performance of each GCM can be seen in Fig. S4. The GFDL-ESM2M model always deviates distinctly from the other four GCMs, showing a significant decrease in FFR and MFL due to a more intense and large inter-annual variation in streamflow. Most GCMs project a slight change for FFR and MFL over 2046-2065 but a significant increase over 2080-2099. Nevertheless, the advanced trend for MFD exhibits much better agreement. Compared with the projected streamflow, the disagreements of these projected reservoir storage metrics are larger.

TABLE 5

The impoundment period of the TGR is from September to November and the change of reservoir storage metrics are closely related to the change of streamflow in this period. The future MFD is projected to occur earlier, consistent with the significant increasing trend of streamflow in September. The FFR declines slightly in the period of 2046-2065. This is likely due to the small increases or even decreases of streamflow in October and November and also the increase of the inter-annual streamflow variation in September and November. The decrease of the FFR is the main reason for the decline of the MFL, while in some cases with an increase of FFR, MFL increases weakly or even declines, indicating that the reservoir levels in the non-fully filled years are abnormally low. Fig. 7 presents the average storage level in non-fully filled years in the reference period and the future two time slices. It can be seen that the average maximum storage level, as well as the average dry season reservoir level of non-fully filled years, are lower in the future compared to the reference period, indicating that extreme low inflows during the storage period will be more severe.

FIGURE 7

4.3 Projected change in hydropower production

Table 6 shows the projected change in the ensemble mean and range of the hydropower metrics relative to the reference period under different RCPs. The MAP generally increases in the two future time horizons and its inter-annual variation increases in most situations. The PAR decreases slightly, while the SPW remarkably increases. Nevertheless, it is worth noting that the results show a large spread across the GCMs and RCPs, with no agreement in the direction of change for all metrics except for SPW in 2080-2099. Statistical significance of the changes for each metric (Fig. S2) demonstrates that the increase of MAP is only consistently significant for all GCMs in 2080-2099 under RCP8.5, and the increase of SPW is significant for most GCMs in both time horizons, while the change of PAR is not significant in most situations.

Detailed information on the seasonal variability and performance of each GCM is presented in Fig. 8. Power generation increases mainly in March – May and September and is also notable for October in 2080-2099. Change of the inter-annual variation of power generation is small and concentrated in the rainy season (May – September), but the spilled water significantly increases for all GCMs, indicating an inadequate utilization capacity of the infrastructure. While the inter-annual variation of power generation in the dry season depends on the GCMs, and although the power generation assurance rate increases in January – April for most GCMs, these exhibit large spreads in September – December. Among the GCMs, the GFDL-ESM2M model shows a distinct increase for inter-annual variation of power generation, a decrease for power assurance rate in the dry season, and an increase for spilled water in the rainy season, resulting in a total decrease of power generation. This model represents an extreme case for the impacts of climate change with regard to intensity and fluctuations. On the contrary, the IPSL-CM5A-LR model shows a weak increase or decrease of inter-annual variation of power generation, a slight increase of power assurance rate, and a moderate increase of spilled water, driving an increase of power generation especially in 2080-2099 (seen in Fig. S2). In addition, the HaDGEM2-ES model displays a significant increase in hydropower generation for both time horizons, due to a large increase in the projected streamflow (Fig. S2).

TABLE 6

FIGURE 8

5. Discussion

Climate change can alter the amount and temporal distribution of natural inflow for reservoirs, and thus affect their operational efficiency. Meanwhile, the regulation and operation of reservoirs will also affect the impact of climate change on water resources, thus making its impact more complicated (Ehsani et al., 2017; Giuliani et al., 2016). Therefore, for basins of highly developed and managed, assessing the impacts of climate change depends largely on the local hydraulic infrastructures and their management. Taking TGR as a case study, this study comprehensively evaluates the impact of the climate change on the streamflow and reservoir performance through coupling GCMs output with hydrological models as well as detailed reservoir operation scheme, and specifically gives concrete insight into how climate change affects hydrological regimes and hydropower output under reservoir operation.

The projected future changes of hydropower for the TGR in this study are generally consistent with findings from Turner et al. (2017b), who projected a 3.5-5.2% increase of hydropower for China (mainly in the south) by the end of 21st with a detailed reservoir operation model. However, the opposite trend is found when compared with a previous study by Liu et al. (2016), which projected a loss in hydropower as a result of the projected decrease in streamflow. It is obvious that dissimilar results may be obtained by different data sources and models used, and highlights the need to reveal the mechanism of hydropower response to climate change, which will be discussed below.

5.1 Response of streamflow to climate change

This study shows that the basin mean temperature is projected to increase by 1.5-5.4^{o}C and precipitation is projected to increase by 4.1-11.7% in the TGR basin by the mid and late 21st century. The simulated annual average streamflow and the extreme high and low flows are all expected to increase. Generally, most previous studies have shown that change of streamflow is consistent with that of precipitation in the study region (Zhang et al., 2018; Chen et al., 2017; Su et al., 2017; Sun et al., 2013). In this study, the response of streamflow to precipitation is roughly linear, for each 10% increase of precipitation, streamflow increases by 15% (Fig. 9). This is consistent with the results by Birkinshaw et al. (2017), which showed that for every 10% increase in precipitation, simulated streamflow increased by 18.7%. However, there is a relatively weak response of streamflow (evapotranspiration) to temperature increase in our study (only results in a 2.2% decrease of streamflow). This is comparable with the observed small decreasing trend of actual evapotranspiration under historical climate change in the past 60 years (Wang et al., 2007). While this was as high as 19% in the study by Birkinshaw et al. (2017), a similar phenomenon of decreased streamflow caused by strong increases of evapotranspiration is also observed from Liu et al. (2016). Despite the changes in the quantity, this study shows an increase in the inter-annual variation of streamflow, in accordance with that of precipitation, which is also revealed by Zhang et al. (2018) for the Yangtze River.

FIGURE 9

5.2 Response of hydropower generation to streamflow change

5.2.1 Influence of seasonal differences

In this study, the annual and monthly average streamflows in the TGR basin are projected to increase in the middle and late 21st century, leading to an overall increase in power generation. The operation schedule of the TGR, however, differs distinctly from flood season to dry season. Therefore, the influence of streamflow change in each season on the reservoir performance is different. Autumn is the critical period for the TGR's impounding. The significant increase of projected streamflow in September improves the FFR and brings forward the average MFD, which is conducive to improving the capacity of the TGR to replenish the downstream flows and generate power during the dry season. On the contrary, under the condition of insufficient inflow causing the reservoir to not be fully filled in autumn, the operational efficiency of the reservoir in the following whole dry season will be affected (Fig. 10). Therefore, the condition of impoundment in autumn can profoundly influence the total reservoir benefit over a year. In the spring, the reservoir is usually at a high operating level and allows the hydropower facility to operate at high efficiency. As a result, increases in spring streamflow will dramatically increase power generation. Due to the low operating level in the flood season, the low generating efficiency of turbines, and the limitation of installed capacity, the increase of power generation caused by increased streamflow is limited. In the winter dry season, since the normal streamflow is relatively low, the impact on the power generation is relatively small. This study for the first time evaluates the impact of hydrological changes on TGR operation by season, which helps to understand the potential benefits of the TGR scheduling management in future climate change scenarios and the necessity of adapting to climate change.

5.2.2 Influence of extreme flow

This study projects that the extreme high flow rate in the TGR basin increases significantly in the mid and late 21st century, indicating more severe flooding in the future. For a flood peak within a limited magnitude and time interval, the TGR can effectively impound the flood to avoid downstream damage. In the case when the streamflow from upstream is too concentrated, however, preparations should be made for the next peak regulation event. This will require the TGR to release a large amount of water that may exceed the maximum flow rate of the turbines, resulting in abandoned (spilled) water. Consequently, the utilization rate of water resources is reduced. In addition, the operating water level of TGR at the present stage can rise 1.5 m above the flood limit of 145 m when there is no flood during flood season, which can significantly improve the efficiency of power generation (Zhou et al., 2018). However, with the increase of extreme high flows in the future, flood control services provided by the TGR will become more important, requiring greater flood storage capacity. As a result, the operating water level of TGR will be further lowered, leading to a decrease in power generation efficiency. On the other hand, although the projected annual extreme low flow has a slight increasing trend, the inter-annual variation of streamflow also increases, especially in the impounding stage. Consequently, although the fully filled rate is slightly increased and the average initial time to reach the normal storage level occurs earlier, the storage level in the years where the reservoir is not fully filled is abnormally low. This leads to the decline of the multi-year mean water level and a decrease in assurance rate and reliability of power generation. The projected change in inter-annual variability of power generation suggests that new operational schemes at the TGR and in upstream reservoirs may be required to sustain required generation.

FIGURE 10

FIGURE 11

5.2.3 Influence of the time scale of hydropower model

For the sake of flood control, the TGR scheduling cannot ensure the maximum utilization efficiency of water resources, and the extreme low flow in a dry year may cause power generation to cease during certain days. Therefore, the response of power generation to streamflow is expected to be non-linear. Fig. 11a shows the response of annual power generation to annual streamflow based on the accumulation of daily power generation obtained by equation (4) and reservoir inflow. It can be seen that when the annual streamflow is 25% higher or 30% lower than the average in the reference period, the power generation is lower than the 1:1 line, indicating that our study using a detailed reservoir model run at the daily scale well captured the nonlinear response mechanism. However, if the daily inflow is synthesized into monthly for calculation of hydropower, the response relationship is generally linear, with a slight deviation only when the streamflow is over 70% higher than average (Fig. 11b). This occurs since a monthly scale model does not reflect the decrease in water utilization efficiency with extreme flow. Based on the monthly scale model, the average power generation in 2046-2065 will be overestimated by 2.4%, and that in 2080-2099 will be overestimated by 4.3%, which may be considered as the maximum increase potential after fully adapting to climate change. Many large scale studies assume a linear relationship between hydropower production and streamflow. For example, Kao et al. (2015) and Bartos (2015) assessed the effects of climate change on hydropower in the United States by regressing power generation on streamflow, which is appropriate at the macro scale, but may overestimate the efficiency of water utilization for a particular reservoir hydropower station. As flood control is the first priority of many large hydraulic infrastructures in China, this study provides valuable reference for further exploration of other facilities as well as regional and national hydropower assessment.

5.3 Uncertainties of the study

This study employs three typical RCPs and five GCMs from CMIP5, which have been proven to capture a large fraction of the full range of CMIP5 projections (Mcsweeney and Jones, 2016). This provides a wide range of hydrological projections in this study area, allowing for drawing more robust conclusions about uncertainty for the impact assessment of hydropower. However, considerable bias exists in the statistical downscaling procedure with WATCH, as well as the mismatch of gridded data in calibrating the hydrological model with CN05.1 since WATCH does not cover the calibration period. As shown in Fig. S5, compared with CN05.1, WATCH underestimates the precipitation by 11.1%, and the downscaling of the five GCMs based on WATCH further lowered the precipitation by 1.1-8.8%, lowered the simulated streamflow by 3.0-21.1%. However, the systematic errors were considered during the two-step regulation process of upstream reservoirs by introducing a scaling factor in the seasonal adjustment model. As a result, the difference in FDC curve of the reservoir inflow for different climate forcing data is significantly reduced (Fig. S5), which would have little effect on the simulation of reservoir regulation and power generation. Nevertheless, under the future scenario, the simulated maximum inflow can reach 100,000 (NorESM1-M)-165,000 (GFDL-ESM2M) m^3/s (Fig. S6), which is about twice the maximum flow in the reference period (1986-2005). While, in the past 1,000 years, the largest flood in the TGR basin occurred in 1870, with a peak flow of about 105,000 m^3/s (Liu et al., 2011). Therefore, there may be large uncertainty in the simulated extreme high flow. The simulation bias of extreme streamflow has little effect on the study of total water resources, but it is very important to the evaluation of reservoir regulation and power generation.

Whilst this study uses only one hydrological model (SWAT), it has been proven that SWAT performs as well as other hydrological models in the study area (Su et al., 2017). The average error of annual streamflow simulation results was less than 5% among the four hydrological models (Chen et al., 2017), which is smaller than that of the GCMs. However, the projected extreme low flow in this study shows a weak increasing trend, while it has been pointed out by other studies that there is a relatively higher uncertainty from hydrological models for lowflow simulation than that for high flow (Giuntoli et al., 2015; Chen et al., 2017).

There is also substantial uncertainty in reservoir regulation. There are hundreds of reservoirs in the upstream of the TGR, therefore the river streamflow in the basin has been artificially altered to a large degree (Zhang et al., 2012). Due to the complexity in joint operation of cascade reservoirs and difficulties in data collection, this study did not consider the impact of reservoir operation on river streamflow in the SWAT simulation but adopted a static empirical correction method. However, as the streamflow volume varies in different years, the reservoir operation changes correspondingly. Therefore, this empirical relationship may not be stable across years, which introduces substantial uncertainty for the simulation of the inflow of the TGR. In the future, the operation and management of the TGR and the upstream reservoirs may change to cope with new requirements and changing environmental conditions due to climate change, which are not considered in this study. In addition, the flood storage capacity of reservoirs in the upstream will increase to double that of current levels according to the long-term construction plan (Zhou et al., 2017). By the time of their completion, the constraint for flood control for the TGR will decrease during the flood season. This may reduce spilled water and result in more usable flood resources and power production. Assuming that the abandoned water can be fully utilized after the coordinated, joint operation of upstream reservoirs, the estimated results of the monthly scale model in Section 5.2 indicates that the power generation in the middle of the 21st century will increase by about 4.4-4.7% compared to current levels, and further increase by 9.5-12.4% at the end of the 21st century. This is likely to be the best result that can be obtained after considering adaptation to climate change.

6. Conclusions

The TGR is a well-known, large-scale water conservancy project in China and the world that provides comprehensive benefits of flood control, power generation, and navigation which will be affected by climate change. In this study, a hydrological model was driven by the climate change projections of five GCMs under three RCPs to simulate the change of natural streamflow in the TGR basin under climate change. The simulated streamflow was revised for upstream reservoir regulation by an empirical method. Subsequently, based on the dynamic simulation of reservoir operation and hydropower facilities, the comprehensive impact of climate change on the inflow, water storage, and power generation of TGR in the middle and late 21st century was systematically assessed. The role and vulnerability of the large-scale water conservancy project in changing the impact of climate change on water resources were revealed.

It is projected that compared to the reference period of 1986-2005, the average annual streamflow, flood season flow, Q5 high flow, and Q95 low flow in the TGR basin will increase in the periods of 2046-2065 and 2080-2099. However, the inter-annual variation of streamflow will increase, and there are wide spreads across GCMs and RCPs, implying large uncertainties inherent in the projections. As a result, the performance of the reservoir changes but with inconsistent trends. The average time to reach the normal storage level in the impounding stage is likely to be advanced, however, the fully filled rate exhibits an increase in 2080-2099 but a decline in 2046-2065, and the mean storage level in the dry season decline for both time horizons. Assuming that future reservoir regulation remains unchanged from the present situation, it is estimated that the annual average power generation will increase by 2.0-2.3% in 2046-2065 and by 5.2-8.1% in 2080-2099, occurring mainly in the spring before the flood season and the early autumn during the end of the flood season. However, the change is only statistically significant in the latter time horizon, and the inter-annual variation of power generation increases especially in the dry season. At the same time, the power generation assurance rate in the dry season exhibits a weak increase or decrease, but spilled water significantly increases in the flood season. If adaptation measures are taken to prevent the occurrence of spilling, the maximum gain of power generation due to climate change in 2046-2065 is 4.4-4.7% and that is 9.5-12.4% in 2080-2099.

Overall, this study highlighted the role of large storage reservoir operations in reshaping impact of climate change on water resources utilization. Firstly, the comprehensive benefits of the reservoir are most sensitive to the inflow during the impounding period. Secondly, the increase of streamflow significantly improves power generation in the dry season. Finally, the increase of streamflow in the flood season does not necessarily yield increased power generation depending on the capacity and utilization efficiency of reservoirs. This is particularly prominent in the monsoon climate region due to the high temporal concentration and large inter-annual variability of precipitation and streamflow. Meanwhile, the reservoir management also increases the uncertainty in assessing the impact of future climate change (Giuliani et al., 2016; Turner et al., 2017a).

In addition, this study has highlighted the increasing trend of extreme hydrological processes and their effect on reservoir performance. Extreme hydrological events, on the one hand, lead to an increase of flood control pressure and difficulty of reservoir management. On the other hand, these events reduce the utilization efficiency of water resources, leading to the non-linear response of hydropower output to climate change. The assessment of this effect requires climate and hydrological information with a high temporal resolution, as well as meticulously capturing reservoir operation. However, the projection of extreme hydrological processes is currently a significant challenge facing the scientific community. Although an increasing number of studies show that the intensity and frequency of extreme precipitation and streamflow on a global scale will increase in the future, great uncertainty still exists in the exact nature and magnitude, and the uncertainty in projection of extreme streamflow is markedly greater than that in the projection of average streamflow (Sillmann et al., 2013; Mohammed et al., 2017).

These findings indicate that the water resources management of the TGR and upstream basin must take corresponding adaptive measures in the future, in order to make use of flood water and cope with the risk of increased inter-annual fluctuation of inflow during the impounding period. Increasing the flood storage capacity and strengthening the joint operation of the upstream cascade reservoirs are important means to overcome these adverse effects and are expected to turn adverse effects into favorable ones. The next step is to strengthen the research on the integrated management strategy of water resources in the upstream of TGR under climate change.

Data availability

Climate change projections of the five GCMs are publicly available from the Inter-Sectoral Impact Model Intercomparison Project (ISI-MIP, https://www.isimip.org). The hydrological and hydropower data for the TGR contain sensitive information for the safety of the dam and cannot be made publicly available. Researchers who wish to conduct studies for this region, however, may contact the corresponding author to discuss the exchange of data.

Acknowledgments

This study was supported by the joint U.S.–China Clean Energy Research Center for Water-Energy Technologies (CERC-WET) project (SQ2018YFE010367, 2016YFE0102400) and the National Key Research and Development Program of China (2018YFE0102400). We also acknowledge the Inter-Sectoral Impact Model Intercomparison Project, which provided climate data of the five GCMs, and the WATCH project, which provided climate forcing data for bias correction of GCMs from 1958 to 2001. Finally, we would like to thank the reviewers for their valuable comments and suggestions, which helped us to improve this manuscript.

References

Arnold, J.G., Srinivasan, R., Muttiah, R.S., Williams, J.R., 1998. Large area hydrologic modeling and assessment part I: model development. Journal of the American Water Resources Association, 34(1): 73-89.

https://doi.org/10.1111/j.1752-1688.1998.tb05961.x.

Bartos, M.D., Chester, M.V., 2015. Impacts of climate change on electric power supply in the Western United States. Nature Climate Change, 5(8): https://doi.org/748.10.1038/nclimate2648.

Berga, L., 2016. The Role of Hydropower in Climate Change Mitigation and Adaptation: A Review. Engineering, 2(3): 313-318. https://doi.org/10.1016/J.ENG.2016.03.004.

Birkinshaw, S.J., Guerreiro, S.B., Nicholson, A., Liang, Q., Quinn, P., Zhang, L., He, B., Yin, J., Fowler, H.J., 2017. Climate change impacts on Yangtze River discharge at the Three Gorges Dam. Hydrol. Earth Syst. Sci., 21(4): https://doi.org/1911-1927.10.5194/hess-21-1911-2017.

Carvajal, P.E., Anandarajah, G., Mulugetta, Y., Dessens, O., 2017. Assessing uncertainty of climate change impacts on long-term hydropower generation using the CMIP5 ensemble—the case of Ecuador. Clim. Change, 144(4): https://doi.org/611-624.10.1007/s10584-017-2055-4.

Chen, L., Frauenfeld, O.W., 2014. A comprehensive evaluation of precipitation simulations over China based on CMIP5 multimodel ensemble projections. Journal of Geophysical Research: Atmospheres, 119(10): 5767-5786. https://doi.org/10.1002/2013jd021190.

Chen, J., Gao, C., Zeng, X., Xiong, M., Wang, Y., Jing, C., Krysanova, V., Huang, J., Zhao, N., Su, B., 2017. Assessing changes of river discharge under global warming of 1.5°C and 2°C in the upper reaches of the Yangtze River Basin: Approach by using multiple- GCMs and hydrological models. Quaternary International, 453: 63-73. https://doi.org/10.1016/j.quaint.2017.01.017.

Chilkoti, V., Bolisetti, T., Balachandar, R., 2017. Climate change impact assessment on hydropower generation using multi-model climate ensemble. Renewable Energy, 109: 510-517. https://doi.org/10.1016/j.renene.2017.02.041.

Deng, H., Luo, Y., Yao, Y., Liu, C., 2013. Spring and summer precipitation changes from 1880 to 2011 and the future projections from CMIP5 models in the Yangtze River Basin, China. Quaternary International, 304: 95-106.

https://doi.org/10.1016/j.quaint.2013.03.036.

de Queiroz, A.R., Marangon Lima, L.M., Marangon Lima, J.W., da Silva, B.C., Scianni, L.A., 2016. Climate change impacts in the energy supply of the Brazilian hydro-dominant power system. Renewable Energy, 99: 379-389. https://doi.org/10.1016/j.renene.2016.07.022.

Ehsani, N., Vörösmarty, C.J., Fekete, B.M., Stakhiv, E.Z., 2017. Reservoir operations under climate change: Storage capacity options to mitigate risk. J. Hydrol., 555: 435-446. https://doi.org/10.1016/j.jhydrol.2017.09.008.

Fan, J.L., Hu, J.W., Zhang, X., Kong, L.S., Li, F.Y., Mi, Z.F., 2018. Impacts of climate change on hydropower generation in China. Mathematics and Computers in Simulation. https://doi.org/10.1016/j.matcom.2018.01.002.

Feng, M., Liu, P., Guo, S., Gui, Z., Zhang, X., Zhang, W., Xiong, L., 2017. Identifying changing patterns of reservoir operating rules under various inflow alteration scenarios. Adv. Water Res., 104: 23-36. https://doi.org/10.1016/j.advwatres.2017.03.003.

Gaudard, L., Romerio, F., Dalla Valle, F., Gorret, R., Maran, S., Ravazzani, G., Stoffel, M., Volonterio, M., 2014. Climate change impacts on hydropower in the Swiss and Italian Alps. Science of The Total Environment, 493: 1211-1221. https://doi.org/10.1016/j.scitotenv.2013.10.012.

Giuliani, M., Anghileri, D., Castelletti, A., Vu, P.N., Soncinisessa, R., 2016. Large storage operations under climate change: expanding uncertainties and evolving tradeoffs. Environmental Research Letters, 11(3). https://doi.org/10.1088/1748-9326/11/3/035009.

Giuntoli, I., Vidal, J.P., Prudhomme, C., Hannah, D.M., 2015. Future hydrological extremes: the uncertainty from multiple global climate and global hydrological models. Earth System Dynamics, 6(1): 267-285. https://doi.org/10.5194/esd-6-267-2015.

Gu, H., Yu, Z., Wang, G., Wang, J., Ju, Q., Yang, C., Fan, C., 2015. Impact of climate change on hydrological extremes in the Yangtze River Basin, China. Stochastic Environmental Research and Risk Assessment, 29(3): 693-707. https://doi.org/10.1007/s00477-014-0957-5.

Guo, X., Huang, J., Luo, Y., Zhao, Z., Xu, Y., 2017. Projection of heat waves over China for eight different global warming targets using 12 CMIP5 models. Theoretical & Applied Climatology, 128(3-4): 507-522. https://doi.org/10.1007/s00704-015-1718-1.

Hempel, S., Frieler, K., Warszawski, L., Schewe, J., Piontek, F., 2013. A trend-preserving bias correction - the ISI-MIP approach. Earth System Dynamics, 4(2): 219-236. https://doi.org/10.5194/esd-4-219-2013.

Huntington, T.G., Weiskel, P.K., Wolock, D.M., McCabe, G.J., 2018. A new indicator framework for quantifying the intensity of the terrestrial water cycle. J. Hydrol. 559, 361-372. https://doi.org/10.1016/j.jhydrol.2018.02.048.

IPCC, 2013. Climate Change 2013: The Physical Science Basis. Contribution of Working Group I to the Fifth Assessment Report of the Intergovernmental Panel on Climate Change. Cambridge University Press, Cambridge. https://doi.org/10.1017/CBO9781107415324.

IPCC, 2014. Climate Change 2014: Impacts, Adaptation and Vulnerability: Part A: Global and Sectoral Aspects: Working Group II Contribution to the IPCC Fifth Assessment Report. Cambridge University Press, Cambridge. https://doi.org/10.1017/CBO9781107415379.

Jahandideh-Tehrani, M., Bozorg Haddad, O., Loáiciga, H.A., 2015. Hydropower Reservoir Management Under Climate Change: The Karoon Reservoir System. Water Resources Management, 29(3): 749-770. https://doi.org/10.1007/s11269-014-0840-7.

Kao, S.-C., Sale, M.J., Ashfaq, M., Uria Martinez, R., Kaiser, D.P., Wei, Y., Diffenbaugh, N.S., 2015. Projecting changes in annual hydropower generation using regional runoff data: An assessment of the United States federal hydropower plants. Energy, 80: 239-250. https://doi.org/10.1016/j.energy.2014.11.066.

Liu, D.F., Xie, B.T., Li, H.J., 2011. Design Flood Volume of the Three Gorges Dam Project. J. Hydrol. Eng., 16(1): 71-80. https://doi.org/10.1061/(Asce)He.1943-5584.0000287.

Liu, L.L., Du, J.J., 2017. Documented changes in annual runoff and attribution since the 1950s within selected rivers in China. Advances in Climate Change Research, 8(1): 37-47. https://doi.org/10.1016/j.accre.2017.03.005.

Liu, L.L., Xu, H.M., Wang, Y., Jiang, T., 2017. Impacts of 1.5 and 2 °C global warming on water availability and extreme hydrological events in Yiluo and Beijiang River catchments in China. Clim. Change, 145(10): 1-14. https://doi.org/10.1007/s10584-017-2072-3.

Liu, X.C., Tang, Q.H., Voisin, N., Cui, H.J., 2016. Projected impacts of climate change on hydropower potential in China. Hydrol. Earth Syst. Sci., 20(8): 3343-3359. https://doi.org/10.5194/hess-20-3343-2016.

Loaiciga, H.A., Valdes, J.B., Vogel, R., Garvey, J., Schwarz, H., 1996. Global warming and the hydrologic cycle. J. Hydrol., 174(1): 83-127. https://doi.org/10.1016/0022-1694(95)02753-X.

Majone, B., Villa, F., Deidda, R., Bellin, A., 2016. Impact of climate change and water use policies on hydropower potential in the south-eastern Alpine region. Science of The Total Environment, 543(Pt B): 965-980. https://doi.org/10.1016/j.scitotenv.2015.05.009.

Maran, S., Volonterio, M., Gaudard, L., 2014. Climate change impacts on hydropower in an alpine catchment. Environmental Science & Policy, 43: 15-25. https://doi.org/10.1016/j.envsci.2013.12.001.

Mcsweeney, C.F., Jones, R.G., 2016. How representative is the spread of climate projections from the 5 CMIP5 GCMs used in ISI-MIP? Climate Services, 1(C): 24-29. https://doi.org/10.1016/j.cliser.2016.02.001.

Mendes, C.A.B., Beluco, A., Canales, F.A., 2017. Some important uncertainties related to climate change in projections for the Brazilian hydropower expansion in the Amazon. Energy, 141: 123-138. https://doi.org/10.1016/j.energy.2017.09.071.

Mohammed, K., Islam, A.S., Islam, G.T., Alfieri, L., Bala, S.K., Khan, M.J.U., 2017. Extreme flows and water availability of the Brahmaputra River under 1.5 and 2 °C global warming scenarios. Clim. Change: 1-17. https://doi.org/10.1007/s10584-017-2073-2.

Naz, B.S., Kao, S.-C., Ashfaq, M., Gao, H., Rastogi, D., Gangrade, S., 2018. Effects of climate change on streamflow extremes and implications for reservoir inflow in the United States. J. Hydrol., 556: 359-370. https://doi.org/10.1016/j.jhydrol.2017.11.027.

Ng, J.Y., Turner, S., Galelli, S., 2017. Influence of El Niño Southern Oscillation on global hydropower production. Environmental Research Letters, 12(3). https://doi.org/10.1088/1748-9326/aa5ef8.

Niu, X., 2016. Key Technologies of the Hydraulic Structures of the Three Gorges Project. Engineering, 2(3): 340-349. https://doi.org/10.1016/J.Eng.2016.03.006.

Rheinheimer, D.E., Viers, J.H., 2015. Combined Effects of Reservoir Operations and Climate Warming on the Flow Regime of Hydropower Bypass Reaches of California's Sierra Nevada. River Research & Applications, 31(3): https://doi.org/269-279. 10.1002/rra.2749.

Savelsberg, J., Schillinger, M., Schlecht, I., Weigt, H., 2018. The Impact of Climate Change on Swiss Hydropower. Sustainability, 10(7): 2541. https://doi.org/10.3390/su10072541.

Shang, Y., Lu, S., Ye, Y., Liu, R., Shang, L., Liu, C., Meng, X., Li, X., Fan, Q., 2018. China' energy-water nexus: Hydropower generation potential of joint operation of the Three Gorges and Qingjiang cascade reservoirs. Energy, 142: 14-32. https://doi.org/10.1016/j.energy.2017.09.131.

Sillmann, J., Kharin, V.V., Zwiers, F.W., Zhang, X., Bronaugh, D., 2013. Climate extremes indices in the CMIP5 multimodel ensemble: Part 2. Future climate projections. J. Geophys. Res. Atmos., 118(6): 2473-2493. https://doi.org/10.1002/jgrd.50188.

Su, B., Huang, J., Zeng, X., Gao, C., Jiang, T., 2017. Impacts of climate change on streamflow in the upper Yangtze River basin. Clim. Change, 141(3): 1-14. https://doi.org/10.1007/s10584-016-1852-5.

Sun, J.L., Lei, X.H., Tian, Y., Liao, W.H., Wang, Y.H., 2013. Hydrological impacts of climate change in the upper reaches of the Yangtze River Basin. Quaternary International, 304(447): 62-74. https://doi.org/10.1016/j.quaint.2013.02.038.

Sun Z.Y., Li C., Liu X.Z., 2012. Estimation of Water Loss for Three Gorges Reservoir. China Three Gorges Construction. 68-69 (in Chinese).

Syed, T.H., Famiglietti, J.S., Chambers, D.P., Willis, J.K., Hilburn, K., 2010. Satellite-based global-ocean mass balance estimates of interannual variability and emerging trends in continental freshwater discharge. Proc. Natl. Acad. Sci. U. S. A., 107(42): 17916-17921. https://doi.org/10.1073/pnas.1003292107.

Tarroja, B., Aghakouchak, A., Samuelsen, S., 2016. Quantifying climate change impacts on hydropower generation and implications on electric grid greenhouse gas emissions and operation. Energy, 111: 295-305. https://doi.org/10.1016/j.energy.2016.05.131.

Turner, S.W.D., Ng, J.Y., Galelli, S., 2017a. Examining global electricity supply vulnerability to climate change using a high-fidelity hydropower dam model. Science of The Total Environment, 590-591: 663-675. https://doi.org/10.1016/j.scitotenv.2017.03.022.

Turner, S.W.D., Hejazi, M., Kim, S.H., Clarke, L., Edmonds, J., 2017b. Climate impacts on hydropower and consequences for global electricity supply investment needs. Energy, 141: 2081-2090. https://doi.org/10.1016/j.energy.2017.11.089.

van Vliet, M.T.H., Wiberg, D., Leduc, S., Riahi, K., 2016. Power-generation system vulnerability and adaptation to changes in climate and water resources. Nature Climate Change, 6: 375. https://doi.org/10.1038/nclimate2903.

Vicuña, S., Dracup, J.A., Dale, L., 2011. Climate change impacts on two high-elevation hydropower systems in California. Clim. Change, 109(1): 151-169. https://doi.org/10.1007/s10584-011-0301-8.

Wang, Y., Jiang, T., Bothe, O., Fraedrich, K., 2007. Changes of pan evaporation and reference evapotranspiration in the Yangtze River basin. Theoretical & Applied Climatology, 90(1-2): 13-23. https://doi.org/10.1007/s00704-006-0276-y.

Wang, Y., Liao, W., Ding, Y., Wang, X., Jiang, Y., Song, X., Lei, X., 2015. Water resource spatiotemporal pattern evaluation of the upstream Yangtze River corresponding to climate changes. Quaternary International, s 380–381: https://doi.org/187-196. 10.1016/j.quaint.2015.02.023.

Woldemeskel, F.M., Sharma, A., Sivakumar, B., Mehrotra, R., 2014. A framework to quantify GCM uncertainties for use in impact assessment studies. J. Hydrol., 519: 1453-1465. https://doi.org/10.1016/j.jhydrol.2014.09.025.

Wu, J., Gao, X.J., 2013. A gridded daily observation dataset over China region and comparison with the other datasets. Chinese Journal of Geophysics, 56(4): 1102-1111 (in Chinese).

Xiong, L.H., Guo, S.L., 2004. Trend Test and Change-Point Detection for the Annual Discharge Series of the Yangtze River at the Yichang Hydrological Station. Hydrological Sciences Journal, 49(1): 99-112.

Xu, H., Taylor, R.G., Xu, Y., 2011. Quantifying uncertainty in the impacts of climate change on river discharge in sub-catchments of the River Yangtze and Yellow Basins, China. Hydrology & Earth System Sciences, 15(1): 333-344. https://doi.org/10.5194/hess-15-333-2011.

Young, G.K., 1967. Finding Reservoir Operating Rules. Journal of the Hydraulics Division, 93(6): 297-322.

Zhang, N., He, H.M., Zhang, S.F., Jiang, X.H., Xia, Z.Q., Huang, F., 2012. Influence of Reservoir Operation in the Upper Reaches of the Yangtze River (China) on the Inflow and Outflow Regime of the TGR-based on the Improved SWAT Model. Water Resources Management, 26(3): 691-705. https://doi.org/10.1007/s11269-011-9939-2.

Zhang, X.J., Tang, Q.H., Liu, X.C., Leng, G.Y., Di, C.L., 2018. Nonlinearity of Runoff Response to Global Mean Temperature Change Over Major Global River Basins. Geophys. Res. Lett., 45(12): 6109-6116. https://doi.org/10.1029/2018gl078646.

Zhang, Y., Gu, A., Lu, H., Wang, W., 2017. Hydropower Generation Vulnerability in the Yangtze River in China under Climate Change Scenarios: Analysis Based on the WEAP Model. Sustainability, 9(11): 2085. https://doi.org/10.3390/su9112085.

Zhang, Y., Zhong, P.-a., Wang, M., Xu, B., Chen, J., 2016. Changes identification of the Three Gorges reservoir inflow and the driving factors quantification. Quaternary International, 475: 28-41. https://doi.org/10.1016/j.quaint.2016.02.064.

Zhou, X.C., Xu, Y.S., Feng, B.F., 2017. An exploration on the interoperability of the flood control capacities of cascade reservoir groups in the upper reaches of Yangtze River. Advances in Water Science, 28(3): 421-428 (in

Chinese).

Zhou, Y., Guo, S., Chang, F., Liu, P., Chen, A.B., 2018. Methodology that improves water utilization and hydropower generation without increasing flood risk in mega cascade reservoirs. Energy, 143: 785-796. https://doi.org/10.1016/j.energy.2017.11.035.

Zhou, Y., Hejazi, M., Smith, S., Edmonds, J., Li, H., Clarke, L., Calvin, K., Thomson, A., 2015. A comprehensive view of global potential for hydro-generated electricity. Energy & Environmental Science, 8(9): 2622-2633. https://doi.org/10.1039/c5ee00888c.

Zhou, B.T., Wen, Q.H., Xu, Y., Song, L.C., Zhang, X.B., 2014. Projected Changes in Temperature and Precipitation Extremes in China by the CMIP5 Multimodel Ensembles. J. Clim., 27(17): 6591-6611. https://doi.org/10.1175/Jcli-D-13-00761.1.

Fig. 1 Location of the TGR and upstream basin as well as the main hydrological stations

Fig. 2 Operating rule curves of the TGR: I, flood control stage; II, impounding stage; III, normal pool level stage; IV, falling stage

Fig. 3 Comparison of simulated and observed hydrographs of monthly reservoir inflow for the TGR

Fig. 4 Flow duration curve of observed, SWAT simulated and regulated daily reservoir inflow for the TGR

Fig. 5 Comparison of simulated and observed annual power generation

Fig. 6 Projected changes in monthly (a) mean streamflow and (b) coefficient of variance for two future time horizons under three RCPs across five GCMs (relative to 1986-2005)

Fig. 7 Reservoir levels for non-fully filled years of five GCMs for two future time horizons and reference period under three RCPs

Fig. 8 Projected changes in monthly (a) power generation, (b) coefficient of variance, (c) assurance rate and (d) spilled water rate for two future time horizons under three RCPs across five GCMs (relative to 1986-2005)

Fig. 9 Projected response of changes in future horizon average of river discharge to precipitation across all GCMs and RCPs (relative to 1986-2005)

Fig.10 Comparison of (a) reservoir water level and (b) power generation between the fully filled year and not

Fig. 11 Response of annual power generation change to annual streamflow change across all GCMs and RCPs (relative to 1986-2005) (a) based on the daily discharge and hydropower model adopted in this study, (b) based on monthly discharge

TABLES

Table 1: Mean monthly inflow, water height, and power generation for Three Gorges reservoir (2013-2017)

Month	Jan	Feb	Mar	Apr	May	Jun	Jul	Aug	Sep	Oct	Nov	Dec
Inflow (m^3/s)	5436	5082	6103	8803	10658	17360	25127	20256	22208	15508	8928	6218
Water height (m)	171.6	168.3	164.9	163.6	155.4	146.7	149.7	148.7	159.1	171.4	174.3	173.6
Power generation (TWh)	4.4	4.2	4.5	6.1	7.7	9.3	13.0	10.5	10.7	8.6	6.3	4.7

Table 2: Summary of the magnitude of the projected climate change at the study region under three RCPs across five GCMs (relative to 1986–2015). The bracketed values indicate the minimum and maximum values for the corresponding parameters.

Period	RCP2.6		RCP4.5		RCP8.5	
	Precipitation (%)	Temperature (°C)	Precipitation (%)	Temperature (°C)	Precipitation (%)	Temperature (°C)
2046-2065	4.6(1.8,7.5)	1.7(0.9,2.4)	4.1(1.3,6.7)	2.2(1.7,2.8)	5.3(3.0,8.3)	3.0(2.0,3.7)
2080-2099	6.0(2.1,10.7)	1.5(1.0,2.0)	9.2(7,12.7)	2.8(1.8,3.4)	11.7(3.2,19.5)	5.4(3.8,6.5)

Table 3: Goodness of fit for SWAT simulation in monthly river discharge above TGR of Yangtze River

Period	Metrics	Pingshan	Gaochang	Beibei	Wulong	Cuntan	Yichang
Calibration	NSE	0.86	0.85	0.85	0.86	0.89	0.87
	R^2	0.87	0.91	0.88	0.89	0.9	0.9
Validation	NSE	0.91	0.83	0.81	0.89	0.87	0.84
	R^2	0.92	0.89	0.88	0.92	0.92	0.92

Table 4: Projected changes in ensemble mean and the ranges of streamflow in TRG under three RCPs and five GCMs (relative to 1986–2015, MAF: mean annual flow, MFF: mean flood season flow, Q_5: high flow, Q_{95}: low flow). The bracketed values indicate the minimum and maximum values for the corresponding parameters.

RCPs	2046-2065				2080-2099			
	MAF (%)	MFF (%)	Q_5 (%)	Q_{95} (%)	MAF (%)	MFF (%)	Q_5 (%)	Q_{95} (%)
RCP2.6	5.6 [0.6,10]	5.8 [-2.9,14.0]	6.9 [-2.5,14.4]	1.3 [-2.9,4.2]	7.9 [3.5,15.8]	8.6 [5.3,17.9]	11.1 [6.9,21]	1.6 [-5,7.1]
RCP4.5	3.3 [1.3,5.7]	3.6 [0.9,7.3]	5.2 [-1.2,11.3]	1.4 [-8.2,6.9]	12.2 [7.2,19]	12.9 [5.2,22.1]	15.3 [8.1,24]	4.5 [-0.6,11.6]
RCP8.5	5.4 [2,12.3]	6.0 [1.3,14.3]	10.1 [5.3,22.9]	0.8 [-5.3,4.4]	15.2 [3.6,32.1]	17.7 [8.8,37.1]	25.5 [12.5,49.8]	2.9 [-6.2,12.3]

Table 5: Projected changes in reservoir storage metrics under three RCPs and five GCMs for TGR (relative to 1986–2015; FFR: fully filled rate, MFD: mean first fully filled day, MFL: mean fill level). The bracketed values indicate the minimum and maximum values for the corresponding parameters.

Period	RCP2.6			RCP4.5			RCP8.5		
	FFR (%)	MFD (day)	MFL (m)	FFR (%)	MFD (day)	MFL (m)	FFR (%)	MFD (day)	MFL (m)
2046-2065	-1.7 [-15,10]	-2.0 [-14.0,8.4]	-0.5 [-1.9,0.3]	-6.7 [-40,11.3]	-4.7 [-10.2,0.9]	-0.6 [-2.2,0.3]	-0.7 [-15,15]	-2.7 [-8.4,5.6]	-0.2 [-1.5,0.3]
2080-2099	4.3 [-25,26.3]	-2.6 [-12.6,3.8]	-0.2 [-2.0,0.6]	3.3 [-3.7,10]	-6.2 [-16.9,-1.0]	-0.2 [-0.3,0.1]	7.3 [-20,26.3]	-8.4 [-20.2,-1.3]	-0.1 [-1.9,0.7]

Table 6: Projected changes in power generation under three RCPs and five GCMs for TGR (relative to 1986–2015; MAP: mean annual power, APR: assurance rate of power generation, AWR: abandoned water ratio). The bracketed values indicate the minimum and maximum values for the corresponding parameters.

RCPs	2046-2065				2080-2099			
	MAP (%)	CV (%)	APR (%)	AWR (%)	MAP (%)	CV (%)	APR (%)	AWR (%)
RCP2.6	2.3	6.2	-0.6	2.1	5.2	-1.1	-0.2	2.9
	[-3.5,8.1]	[-1.4,23.8]	[-.4,2.9]	[-0.4,6.6]	[-5.8,9.7]	[-6.7,7.3]	[-5.7,2.8]	[0.6,5.8]
RCP4.5	0.9	2.5	-0.8	1.9	7.9	7.3	-0.1	4.0
	[-12.1,5.7]	[-5.9,8.6]	[-.1,2.7]	[-0.5,6.0]	[2.0,11.5]	[4.2,9.1]	[-1.0,1.0]	[1.6,7.0]
RCP8.5	2.0	3.7	-0.3	3.0	8.1	0.9	-0.2	6.2
	[-2.9,6.0]	[-1.6,6.6]	[-.9,1.0]	[-0.1,4.4]	[-11,16.8]	[-7.4,12.9]	[-8.6,3.6]	[3.7,10.1]

Declaration of interests

☒ The authors declare that they have no known competing financial interests or personal relationships that could have appeared to influence the work reported in this paper.

☐The authors declare the following financial interests/personal relationships which may be considered as potential competing interests:

1) The annual power generation of TGR will increase under climate change.

2) The stability of power generation of TGR will decrease.

3) The response of TGR power generation to streamflow change is non-linear due to hydrological extremes.

4) The future reservoir management for TGR should take adaptive measures to deal with the flood and reduce the spilled water.